Available online at www.sciencedirect.com

SCIENCE DIRECT®

Ecological Modelling 187 (2005) 232–246

ECOLOGICAL MODELLING

www.elsevier.com/locate/ecolmodel

# Modelling macroalgae using a 3D hydrodynamic-ecological model in a shallow, temperate estuary

A.R. Trancoso*, S. Saraiva, L. Fernandes, P. Pina, P. Leitão, R. Neves

*Maretec, Instituto Superior Técnico, Av. Rovisco Pais, 1049-001 Lisboa, Portugal*

Received 26 June 2003; received in revised form 17 June 2004; accepted 27 January 2005

## Abstract

This paper describes an application of MOHID modelling system to a shallow temperate coastal lagoon in Portugal's western coast (Ria de Aveiro), simulating more than one primary producer, for a better understanding of the existing ecological dynamics and creating a useful tool to delineate land activities management practices. MOHID water quality model is driven by a physical transport model and simulates the dynamics and productivity of the two main primary producers (phytoplankton and macroalgae) as well as the cycling of nitrogen, carbon and oxygen in interaction with sediment and hydrodynamics. The integrated model is forced by exchanges with the Atlantic Ocean (tide), atmosphere, and by sediment and nutrient inputs from the upstream rivers and other discharges. Focus is given to the light parameterization of primary production, influence of hydro and sediment dynamics and to the prediction of seaweed beds distribution. The results obtained show that the model is better adjusted to field data with macroalgae's simulation and that macroalgae can have an important role in primary production. Hydrodynamic conditions can be significant in the competition between the two primary producers, determining the predominant groups as well as their limiting factors.

*Keywords:* Modelling; Macroalgae; Phytoplankton; Nutrients; Sediment; Coastal lagoon

## 1. Introduction

Estuaries are often eutrophic systems due the nutrient inputs from land activities and runoff. Since they are coastal waters, they benefit from low depths associated with high water mixing being characterized by high biological activity. They are often heavily populated areas increasing the pressure on the quality status of waters and the need for proper management strategies (Valiela, 1995; Carr et al., 1997). Nutrient enrichment can alter the structure of the ecosystem and to deal with the consequences (high water turbidity, toxic/harmful algal blooms, shifts in species, etc.) one must first understand the role of primary production at the system level (Mann, 1982; Cloern, 2001).

Nutrient uptake during algal growth is the main process of nutrient removal from the water. Photosynthetic oxygen production during daylight and consumption

---

* Corresponding author. Tel.: +351 21 841 9436;
fax: +351 21 421 1272.
*E-mail address:* ana.rosa.maretec@ist.utl.pt (A.R. Trancoso).

0304-3800/$ – see front matter © 2005 Elsevier B.V. All rights reserved.
doi:10.1016/j.ecolmodel.2005.01.054

through respiration during the night can cause great diurnal variations in dissolved oxygen. When there are high loads of nutrients, the system can become over-saturated with biomass producing oxygen and consuming nutrients during the day, supporting great populations of consumers and decomposers. By night, the oxygen is rapidly depleted creating anoxia conditions that disrupt the system resulting in massive fish kills under severe conditions. (Mann, 1982; Parsons et al., 1984; Little and Kitching, 1996)

However, estuary specificities like topography, climate and freshwater discharges modulate the magnitude of processes and their consequences (Day et al., 1989). In deep estuaries, benthic production may have an insignificant contribution in relation to pelagic one, due to light limitation. However, in shallow areas with low mean residence times, benthic producers like macroalgae can compete for nutrients with phytoplankton that do not reside long enough to use the nutrients carried from the upstream rivers or discharges (Braunschweig et al., 2003). Sediment dynamics has also a major role in productivity because it determines the underwater light availability and macroalgae attachment conditions (Portela, 1996; Salomonsen et al., 1999).

Mathematical models that integrate hydrodynamic, sediment transport and major water quality processes can aid in developing hypotheses about the ecosystem dynamics and the possibility of simulating several scenarios (Neves et al., 2000). MOHID is a modelling system that integrates these features and has been widely studied and applied in different estuarine ecosystems: in Tagus estuary (Portela, 1996; Pina et al., 2000, 2003; Pina, 2001; Braunschweig et al., 2003), in Guadiana estuary (Cunha et al., 2000), in Douro estuary (Pina et al., 2003) and in all Portuguese estuaries as part of an official study requested by the Portuguese National Water Institute (INAG, 2003) to determine water quality status contributing to coastal management supported by modelling (following European Council Directives 91/271/EEC and 91/676/EEC). The water quality model in MOHID has been also applied to ocean waters such as in seamounts (Coelho and Santos, 2003), in the western Iberian continental shelf to optimize the level of treatment of urban discharges into coastal waters (Neves et al., 2000).

The modelling system with the pre- and post-processing tools is described by several papers (Miranda et al., 2000; Neves et al., 2000) and thesis (Portela, 1996; Pina, 2001). Recently, macroalgae productivity was included in MOHID. Models that simulate macroalgae dynamics are well reported in the literature (Coffaro and Sfriso, 1997; Solidoro et al., 1997; Duarte and Ferreira, 1997; Alvera-Azcárate et al., 2003; Baird et al., 2003) each one with its own specificities. This paper presents MOHID's primary production parameterizations and its application to a temperate shallow coastal lagoon, to study the influence of benthic macroalgae in the system behaviour, particularly in terms of phytoplankton and nutrient concentrations. Focus is given to the light parameterization of primary production, influence of hydro and sediment dynamics and to the prediction of seaweed beds distribution.

## 2. Methodology

### 2.1. Site description and pre-processing

Ria de Aveiro (being the name commonly attributed to the Vouga Estuary) is a shallow temperate coastal lagoon with extensive intertidal areas. The Ria spreads through nearly 45 km along the occidental coast of Portugal between Ovar and Mira (48°38′N, 8°44′W), and a maximum width of 10 km. The total covered area of the estuary changes between 83 km$^2$ during spring tide and 66 km$^2$ in neap tide (Dias et al., 1999). Average depths are in the order of 1 m, but maximum depths are artificially maintained by dredging varying between 1 and 4 m.

Ria de Aveiro is constituted by five main channels (see Fig. 1), and for each it is possible to consider a fresh water discharge: Vouga River in the Main Channel, Antuã River in Murtosa Channel, Caster River in S.Jacinto/Ovar Channel, Boco River in Ilhavo Channel, and in Mira Channel there are some artificial drains that can be considered as an input of fresh water. These loads represent not only an entrance of fresh water into the estuary, but also an input of nutrients. The WWTPs (Waste Water Treatment Plants) existing in Ria area were not considered in this study because the treated effluents correspond to only 10% of the population, representing about 0.5% of the total input in the estuary (INAG, 2003). Diffuse loads due to agricultural land lixiviation were considered negligible when com-

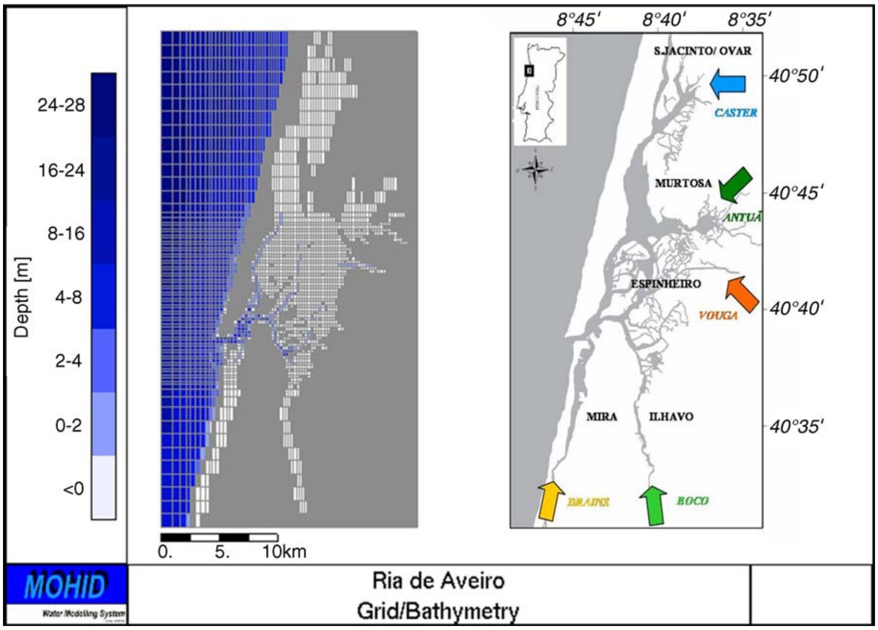

Fig. 1. Ria de Aveiro estuary (left: bathymetry and grid used in model simulations; right: location of Ria de Aveiro and its channels and discharges (in italics).

pared with the contribution of agricultural load carried by rivers.

The hydrodynamic model was forced with a M2 tide at the ocean boundary and considering the annual average discharge of each river shown in Table 1. Values in this table were obtained from statistical analysis of time series records obtained in field stations by INAG (http://snirh.inag.pt).

The computation grid used was 326 × 318 cells wide with a variable spatial step (minimum of 50 m) (see Fig. 1). This resolution was considered fine enough to describe the main physical processes in the Ria, but is not time efficient for long term simulations. For this reason, the ecological processes, that need at least 1 year of simulation, were computed using a different grid, resulting from the spatial integration of bathymetry, merging 4 × 4 grid cells into one. The hydrodynamic conditions were recorded into a file, which can be used as input of the water properties transport model. This file was recorded along a M2 tide period (12 h 25 min 30 s), being repeated along the water quality simulation period, decreasing the computational effort of the model.

Table 1
River discharges in Ria de Aveiro used in hydrodynamic simulations (statistical analysis of time series records obtained in field stations by INAG: http://snirh.inag.pt)

| | |
|---|---|
| Vouga River | 28.8 $m^3/s$ |
| Antuã River | 6.3 $m^3/s$ |
| Caster River | 5 $m^3/s$ |
| Boco River | 2.5 $m^3/s$ |
| Artificial drains in Mira Channel | 3 $m^3/s$ |

Being a shallow estuary, Ria de Aveiro is characterized by the presence of several species of algae and vascular plants, commonly called *moliço*, used by inhabitants in soil fertilizing. The simulation of all photosynthetic organism species present in Ria de Aveiro by MOHID system is not possible yet, but the inclusion of macroalgae processes as an additional primary producer revealed some interesting results. In order to study the impact of macroalgae production in the over all water quality parameters, a comparison between the simulations WITH and WITHOUT macroalgae will be presented in this paper.

### 2.2. Water quality model

To model organic matter cycling, a set of conservation equations are solved for the following state variables: phytoplankton and macroalgae as primary pro-

Table 2
Relevant water quality model parameters used in model simulations

| Variable | Description | Units | Default | Reference |
|---|---|---|---|---|
| Macroalgae | | | | |
| $\mu_{\max}^{\mathrm{MA}}(T_{\mathrm{ref}})$ | Maximum gross growth rate at the reference temperature | $\mathrm{day}^{-1}$ | 0.4 | Coffaro and Sfriso (1997); Coffaro and Bocci (1997) |
| $I_{\mathrm{opt}}$ | Optimum light intensity for macroalgae photosynthesis | $\mathrm{W\,m}^{-2}$ | 90.0 | EPA (1985) |
| $h_{\mathrm{MA}}$ | Average macroalgae bed height | M | 0.25 | Ferreira (1989) |
| $a_{\mathrm{MA}}$ | Carbon specific shading area | $\mathrm{m}^2\,\mathrm{kgC}^{-1}$ | 11.1 | Calibration |
| $K_{\mathrm{N}}^{\mathrm{MA}}$ | Nitrogen half-saturation constant | $\mathrm{mgN\,L}^{-1}$ | 0.065 | EPA (1985), Valiela (1995) |
| $K_{\mathrm{re}}^{\mathrm{MA}}$ | Endogenous respiration constant | $\mathrm{day}^{-1}$ | 0.00175 | EPA (1985), Portela (1996) |
| $K_{\mathrm{e}}^{\mathrm{MA}}$ | Excretion constant | – | 0.008 | Portela (1996) |
| $m_{\max}^{\mathrm{MA}}(T_{\mathrm{ref}})$ | Maximum mortality rate at the reference temperature | $\mathrm{day}^{-1}$ | 0.003 | Portela (1996) |
| $K_{\mathrm{m}}^{\mathrm{MA}}$ | Macroalgae mortality half-saturation rate | $\mathrm{kgC\,m}^{-2}\,\mathrm{day}^{-1}$ | 0.03 | Portela (1996) |
| $G_{\mathrm{MA}}$ | Grazing rate on macroalgae | $\mathrm{day}^{-1}$ | 0.00008 | Valiela (1995) |
| $F_{\mathrm{dep}}^{\max}$ | Maximum deposition flux | $\mathrm{gC\,m}^{-2}\,\mathrm{s}^{-1}$ | 0.005 | Dronkers and Leussen (1988) |
| $\tau_{\mathrm{ero}}^{*}$ | Detachment critical shear stress | Pa | 1 | Salomonsen et al. (1999) |
| Phytoplankton | | | | |
| $\mu_{\max}^{\mathrm{MA}}(T_{\mathrm{ref}})$ | Maximum gross growth rate at the reference temperature | $\mathrm{day}^{-1}$ | 1.8 | Pina (2001) |
| $I_{\mathrm{opt}}$ | Optimum light intensity for phytoplankton photosynthesis | $\mathrm{W\,m}^{-2}$ | 100.0 | EPA (1985) |
| $K_{\mathrm{N}}^{\mathrm{MA}}$ | Nitrogen half-saturation constant | $\mathrm{mgN\,L}^{-1}$ | 0.014 | EPA (1985), Valiela (1995) |
| $K_{\mathrm{re}}^{\mathrm{MA}}$ | Endogenous respiration constant | $\mathrm{day}^{-1}$ | 0.0175 | EPA (1985), Portela (1996) |
| $K_{\mathrm{e}}^{\mathrm{MA}}$ | Excretion constant | – | 0.07 | Portela (1996) |
| $m_{\max}^{\mathrm{MA}}(T_{\mathrm{ref}})$ | Maximum mortality rate at the reference temperature | $\mathrm{day}^{-1}$ | 0.02 | Portela (1996) |
| $K_{\mathrm{m}}^{\mathrm{MA}}$ | Phytoplankton mortality half-saturation rate | $\mathrm{mgC\,L}^{-1}\,\mathrm{day}^{-1}$ | 0.3 | Portela (1996) |
| $E$ | Phytoplankton assimilation efficiency | – | 0.6 | Pina (2001) |
| Common parameters | | | | |
| $\alpha_{\mathrm{N:C}}$ | Macroalgae N:C ratio (Redfield ratio) | $\mathrm{mgN\,mgC}^{-1}$ | 0.18 | Atkinson and Smith (1983), Falkowski (2000) |
| $f_{\mathrm{in}/X}$ | Soluble inorganic fraction of the $X$ excretions | – | 0.25 | Portela (1996) |
| $f_{\mathrm{orgD}/X}$ | Dissolved organic fraction of the $X$ organic excretions | – | 0.25 | Portela (1996) |

ducers, zooplankton as consumer, dissolved nutrients, oxygen, organic matter in the pelagic phase and organic matter in the benthic phase (particulate, refractory and non-refractory). The sinks and sources terms (i.e. the ecological processes) are computed in Water Quality Module of MOHID, giving the model the desired flexibility to be coupled to either a Lagrangian or an Eulerian resolution method (Pina, 2001). The parameterisation of the ecological processes in the water column (pelagic system) is mainly adapted from EPA (1985), with the above mentioned state variables. Only nitrogen and phosphorous cycles are simulated explicitly and therefore, the simulation of organic matter assumes constant C:N:P[1] ratios.

To better understand the interactions between the phytoplankton and macroalgae, a more detailed insight of primary production parameterizations will be presented in the subsequent sections. The default values for the some of the most important model parameters are presented in Table 2.

### 2.2.1. *Primary production*

Since macroalgae and phytoplankton have the same growth requirements (light and nutrients) and are subject to the same basic processes, the same formulations can be used, although the specific values of some coefficients will vary to characterise the difference between the two groups. In addition, due to the morphological characteristics of the two producers, the major differences between them can be summarised in:

- macroalgae are associated with the bottom substrate and are expressed in terms of areal densities ($\mathrm{kg\,m}^{-2}$) rather than volumetric densities or concentrations used for phytoplankton;

---

[1] C—carbon; N—nitrogen; P—phosphorous.

- macroalgae do not have hydrodynamic transport;
- macroalgae have no settling losses, but instead they have additional losses by scouring from the bottom substrate, when bottom shear stress is high;
- macroalgae cannot firmly attach to the substrate in areas characterized by high positive and regular sedimentation rates;
- emerged macroalgae are considered dormant, and the productivity yield after re-immersion is not affected (Bell, 1993).

Following an exponential population growth model, where the temporal variation of biomass depends on the existent biomass (Gotelli, 1995), one can say that primary production of either phytoplankton or macroalgae ($X$) is governed by the equation:

$$\frac{\partial \Phi_X}{\partial t} = (\mu_X - r_X - \mathrm{ex}_X - m_X - G_X)\Phi_X \qquad (1)$$

where $t$ is the time (day), $\Phi_X$ biomass (gC m$^{-3}$ for phytoplankton; kgC m$^{-2}$ for macroalgae) and the others can be seen as the net production rate, composed of: $\mu_X$—the gross growth rate (day$^{-1}$); $r_X$—the total respiration rate (day$^{-1}$); $\mathrm{ex}_X$—the excretion rate (day$^{-1}$); $m_X$—the natural mortality rate (non-predatory) (day$^{-1}$); $G_X$—the grazing rate (day$^{-1}$).

Facilitating result analysis, a simple parameterization was used for gross growth rate. It was defined as a function of water temperature, availability of photosynthetic active radiation (PAR) and nutrients in the water column. The major growth limitation nutrients are nitrogen and phosphorous because carbon is often available in excess, and micronutrients like iron, manganese, etc. are only limitative in oligotrophic systems. The joint dependence of these variables is defined by separate growth limiting factors (function $\psi$ in Eq. (2)), that can range from a value of 0 to 1. A value of 1 means the factor does not limit growth (i.e. light is at optimum intensity, nutrients are available in excess, etc.). The limiting factors are then combined with a maximum gross growth rate at a reference temperature as in the following equation:

$$\mu_X = \mu_{\max}^X(T_{\mathrm{ref}}) \times \Psi(T) \times \Psi(I) \times \min(\Psi(N), \Psi(P)) \qquad (2)$$

where $T$ is the temperature (°C), $I$ the radiation intensity (W m$^{-2}$), $N$ the nitrogen (ammonia and nitrate) concentration (mgN L$^{-1}$) and $P$ the phosphorous concentration (mgP L$^{-1}$). Temperature and light limitation factors follow an inhibition law and nutrient limitation factors follow Michaelis–Menten saturation law. Light limitation factor formulation is based on an integration of Steele photosynthetic response curve within the water column (Pina, 2001) (see Eq. (7)).

The model assumes that growth rates are determined by external concentrations of available nutrients. Therefore, nutrient composition of algal cells remains constant (fixed stoichiometry models) and growth and nutrient uptake rates are linearly dependent. Thus, the assumed C:N:P ratio is the Redfield ratio (106:16:1; average in marine environment) for macroalgae, phytoplankton, zooplankton and non-living organic matter (Atkinson and Smith, 1983; Falkowski, 2000). Although stoichiometric cellular ratios depend on species, cell dimension, external and physiological conditions, most water quality models use the fixed stoichiometry approach because it simplifies the model without prejudice of results, unless one wants to simulate explicitly luxury uptake and nutrient storage in organisms (EPA, 1985; Valiela, 1995). Respiration ($r_{\mathrm{e}}^X$), excretion ($\mathrm{ex}_X$) and mortality ($m_X$) formulations can be seen in EPA reference ecological model (EPA, 1985). Grazing rate on macroalgae is computed by an imposed rate, while for phytoplankton its value depends on zooplankton dynamics (Pina, 2001).

### 2.2.2. Light availability

Photosynthetic organisms only exist where light is able to reach their cells. This means that phytoplankton is limited to the uppermost layers of the water column (photic zone) and that benthic algae are confined to shallow coastal waters where light reaches the bottom. The depth to which photosynthesis will occur is determined mainly by (1) the incident surface radiation, (2) the extinction of light in the water, and (3) the photosynthetic response to light. In the water column, the Lambert–Beer law defines the attenuation of light with depth:

$$I(z) = I_0\,\mathrm{e}^{-kz} \qquad (3)$$

where $I$ (W m$^{-2}$) is the light intensity at a given depth $z$ (m), $I_0$ the light intensity at the surface and $k$ the light extinction coefficient (m$^{-1}$).

The majority of the water quality models reviewed by Parsons et al. (1984), Rivera (1997) and Pina (2001) compute the water column light extinction coefficient considering phytoplankton self-shading effect and particulate suspended material, establishing the following relationship:

$$k = k_{\mathrm{w}} + k_{\mathrm{p}} C_{\mathrm{p}} + k_{\mathrm{s}} C_{\mathrm{s}} \tag{4}$$

where $k$ and $C$ stand for specific light extinction coefficient and concentration, and index w, p and s refer to water, phytoplankton's chlorophyll and total suspended solid in the water column. The different set of parameters to be used should be based on local measurements (specially $k_{\mathrm{s}}$) that allow the determination of the overall extinction coefficient. By applying the Lambert–Beer law, with a given extinction coefficient, one can compute the light available for photosynthesis at a given depth.

In the benthic boundary layer, light will be attenuated mainly by macroalgal *thalli* that exert an intense self-shading effect. The total amount of shading effect depends of the *thalli* density, i.e., biomass density, as well as on macroalgal morphology. Following this and recognising that there are no sufficient in-depth studies of macroalgae's light needs, a somewhat different approach must be undertaken for the light extinction coefficient in the benthic boundary layer. The prevailing light absorbing components will be macroalgae *thalli* and therefore the extinction coefficient must depend on their biomass, height and morphology. The joint dependence of these factors can be adjusted to the state variables of the model resulting in the following relationship:

$$k_{\mathrm{MA}} = \frac{a_{\mathrm{abs}} \times \Phi_{\mathrm{MA}}}{\min(h_{\mathrm{MA}}, h_{\mathrm{WC}})} \times \max\left(\frac{h_{\mathrm{MA}}}{h_{\mathrm{WC}}}, 1\right) \tag{5}$$

where $k_{\mathrm{MA}}$ is the macroalgae bed light extinction coefficient ($\mathrm{m}^{-1}$), $a_{\mathrm{abs}}$ the carbon-specific shading area ($\mathrm{m}^2\,\mathrm{kgC}^{-1}$), $\Phi_{\mathrm{MA}}$ the macroalgal biomass ($\mathrm{kgC\,m}^{-2}$), $h_{\mathrm{MA}}$ the macroalgal bed average height and $h_{\mathrm{WC}}$ the water column height (m). The carbon-specific shading area depends on frond and *thalli* morphology. Macroalgae's carbon-specific absorption cross-section values were determined by Enriquez et al. (1994) and used by Baird et al. (2003) and vary between 11.1 and 145.3 $\mathrm{m}^2\,\mathrm{kgC}^{-1}$ (mean of 54.1 $\mathrm{m}^2\,\mathrm{kgC}^{-1}$) depending on the macroalgal morphology. The carbon-specific shading area accounts only for the surface area that causes shading, and thus, it will be lower than the total surface area given by the values above. An average height for the macroalgal bed was used considering that the more elongated are macroalgae's fronds, the more they will be subject to higher drag and friction forces, increasing the probability of being broken or detached from the substratum. When emerged, even if only partial, the self-shading effect is severely aggravated by the bending of the stipes (Fig. 2) and thus the multiplication by the second factor in Eq. (5).

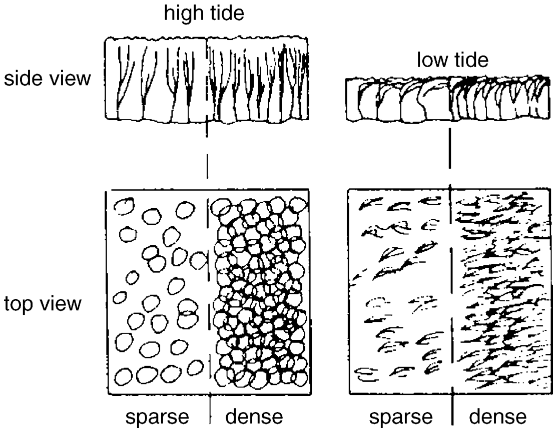

Fig. 2. Top and side views of sparse and dense macroalgae meadows at different tide levels. Side view shows vertical orientation, top view represents the area of overlap. After Dennison (1979) in Fonseca and Kenworthy (1987).

### 2.2.3. Photosynthetic response to light

The relationship of photosynthetic rate to light intensity in macroalgae is similar to that found in single-celled algae (EPA, 1985; Valiela, 1995), and can be defined with Steele photoinhibition law (Steele, 1962):

$$\frac{P}{P_{\max}} = \frac{I}{I_{\mathrm{opt}}} \exp\left(\frac{1 - I}{I_{\mathrm{opt}}}\right) \tag{6}$$

where $P$ is the photosynthetic rate at a given light intensity $I$ ($\mathrm{W\,m}^{-2}$) for an organism that has a maximum photosynthetic rate $P_{\max}$ at the optimal (saturating) light intensity $I_{\mathrm{opt}}$. The light limitation factor used in Eq. (2) is obtained by:

$$\Psi(I) = \int_0^h \frac{P}{P_{\max}}\,\mathrm{d} \tag{7}$$

with $h = h_{\mathrm{WC}}$ for phytoplankton and $h = \min(h_{\mathrm{WC}}, h_{\mathrm{MA}})$ for macroalgae.

### *2.2.4. Macroalgae establishment and distribution*

In contrast with phytoplankton, macroalgae grow attached to substrata and are not transported in the water column unless dislodged or broken by ambient water currents and waves. Yet, they also depend on moving water. Advection and diffusion transport are responsible for dispersing the spores, washing away waste products and sediments, and transport of dissolved materials such as nutrients and gases (Kaandorp and Kübler, 2001). Therefore, determination of macroalgal attachment conditions constitutes a significant factor in macroalgal production patterns.

The breakability effect can be accounted by the definition of macroalgal erosion zones, based on the concept of critical bottom shear stress, establishing an analogy with Partheniades's approach for sediment dynamics (Partheniades, 1965). In this approach, when bottom shear stresses are higher than a critical value, erosion of sediments will occur. In a similar way, when the shear stress acting on attached macroalgae by the water velocity is higher than a critical value, macroalgae will detach and, from this point, considered as particulate non-living matter. According to Salomonsen et al. (1999), critical bottom shear velocities for macroalgal detachment can range from $0.012\,\mathrm{m\,s^{-1}}$ (for small dimension macroalgae) to $0.15\,\mathrm{m\,s^{-1}}$, i.e., from 0.14 to $22.5\,\mathrm{N\,m^{-2}}$ in shear stress units.

On the other hand, macroalgae cannot attach in places where the substrate is sufficiently not rigid, such as the ones subject sediment deposition. In an estuarine system, deposition zones are spatially stable and have typical deposition patterns, not just because of hydrodynamic factors but also due to salinity effects. Sediment dynamics is dependent on hydrodynamic factors (tidal flow and wave action), the nature of the substrate (topography and total sediment load) and salinity (flocculation effects). Hence, deposition fluxes can be given by:

$$F_{\mathrm{dep}} = \frac{\mathrm{d}M_{\mathrm{dep}}}{\mathrm{d}t} = (C\omega_{\mathrm{S}})_{\mathrm{B}}\left(1 - \frac{\tau}{\tau^{*}_{\mathrm{dep}}}\right) \tag{8}$$

where $F_{\mathrm{dep}}$ is the deposition flux ($\mathrm{kg\,m^{-2}\,s^{-1}}$), $M_{\mathrm{dep}}$ the sediment deposited concentration ($\mathrm{kg\,m^{-2}}$), $t$ the time (s), $C$ the near-bed sediment concentration ($\mathrm{kg\,m^{-3}}$), $\omega_{\mathrm{S}}$ the settling velocity ($\mathrm{m\,s^{-1}}$), $\tau$ the bottom shear stress and $\tau^{*}_{\mathrm{dep}}$ the sediment critical deposition shear stress (Krone, 1962). Typical estuarine sediment deposition fluxes are in the order of magnitude of approximately $5 \times 10^{-3}\,\mathrm{g\,m^{-2}\,s^{-1}}$ given by typical settling velocities of magnitude $10^{-4}\,\mathrm{m\,s^{-1}}$, near-bed sediment concentrations of $100\,\mathrm{mg\,L^{-1}}$, and bottom shear stresses of about one half the critical deposition shear stress (Dronkers and Leussen, 1988).

## 3. Results and discussion

In order to provide a better evaluation, the model results can be analyzed for the estuary as a whole, or integrated in different boxes (see Fig. 3c). The integration in boxes allows the comparison of the annual average values obtained from the model results, in the different boxes, with field data values measured in stations located in each box. The boxes were drawn according to the zone of influence of each discharge and the resemblance in water residence time. The stations are represented in Fig. 3a and b. MR stations were performed in the scope of ModelRia project (financed by the Portuguese Science and Technology Foundation) and sampled in June and September of 2000. RA stations correspond to Portuguese Hydrographical Institute (Instituto Hidrográfico) samples, in the scope of a Portuguese estuarine coastal monitoring program. The information is available only in terms of annual average of nutrients and phytoplankton for the years between 1989 and 1993 and for February 2002.

The hydrodynamic results of the simulations in Ria de Aveiro showed that there is an important recirculation inside the estuary, which generates high water mixing from different parts of the estuary. Close to the estuary mouth there is a complete mixing of water, but the residence times of each different part seems to be different. Defining residence time as time required for 80% of the water to leave the Ria, and applying the Lagrangian tracers model of MOHID, the average residence time of Ria de Aveiro was calculated as 20 days. Boxes 1, 3 and 7 (Fig. 3c) are areas with higher residence times, making these areas advantageous for phytoplankton growth because it resides long enough to use the dissolved nutrients. The hydrodynamic results are more deeply analyzed in INAG (2003).

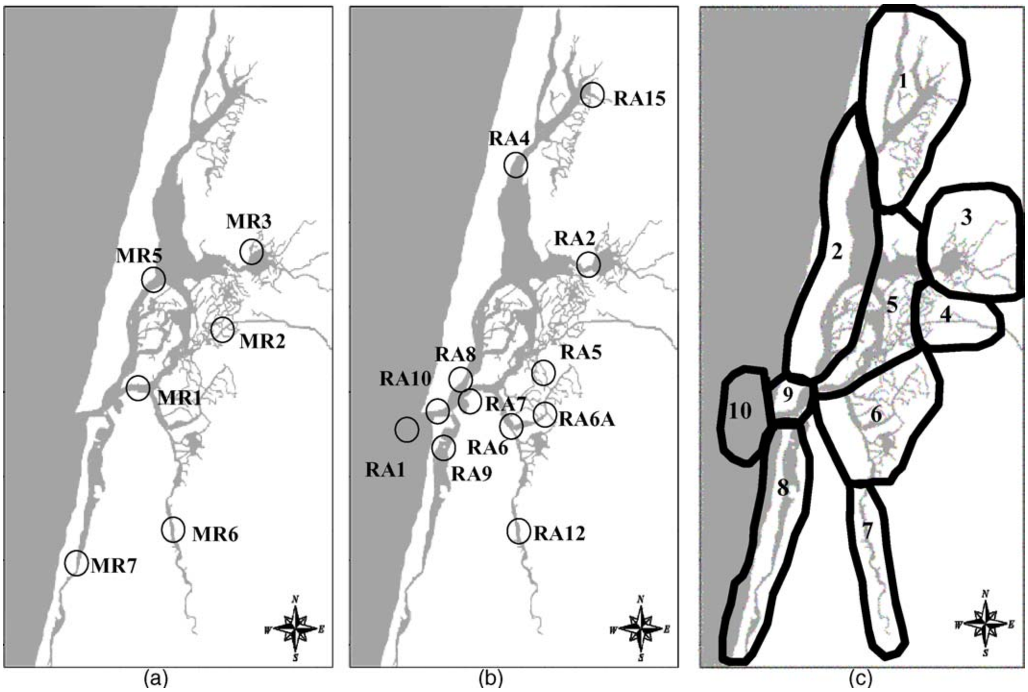

Fig. 3. (a) and (b) Location of sampling stations used to evaluate the results of the model; (c) integration boxes in Ria de Aveiro.

The water quality results allowed the comparison between annual average concentrations of some properties (obtained from model results WITH and WITHOUT macroalgae) and field data records in each box, as represented along Fig. 4. Phytoplankton and zooplankton concentration, obtained in the simulation with macroalgae, is closer to field data records in every box (Fig. 4a and b), indicating that the inclusion of macroalgae improved the model results, regarding phytoplankton and zooplankton biomass. Fig. 4c shows that ammonia concentrations obtained by the model WITH macroalgae are a little lower than WITHOUT macroalgae, but are both within the confidence intervals of field data, except for box 1. This can be explained by a possible underestimation of Caster River's nutrient loads by the model and by the fact that we are comparing punctual station records – see station RA15 in Fig. 3b – with spatially average results in 1.6 km$^2$ (area of box 1). In nitrate results, the differences between the two simulations are quite significant (Fig. 4d). The average concentration values obtained WITH macroalgae are much lower than WITHOUT macroalgae. Comparing with field data records, the results WITH macroalgae seem to be too low and WITHOUT macroalgae the results have a better approximation to the field data. Thus, results can suggest that, either nitrate sources in the system were underestimated or, there is a different source of nitrate in the system that is not being considered in this study, such as underground water contribution. The area surrounding Ria de Aveiro has extensive agriculture systems and field lixiviation (caused by rain or irrigation) can possibly lead nitrate compounds to Ria de Aveiro through surface (rivers) or underground (which is not considered in this study). More detailed studies will be needed to calibrate the model results and conclude about the precision of results regarding this aspect.

The oxygen results (Fig. 4e) WITH macroalgae tend to be, on average, higher than WITHOUT macroalgae, as a result of one more photosynthetic organism present in Ria de Aveiro, increasing oxygen production. These results are also higher than field data records, possibly because the high mixing of water reduces dissolved oxygen concentration. The fact that we are running simulation with a M2 + S2 tide may cause some underestimation of mixing effects in water.

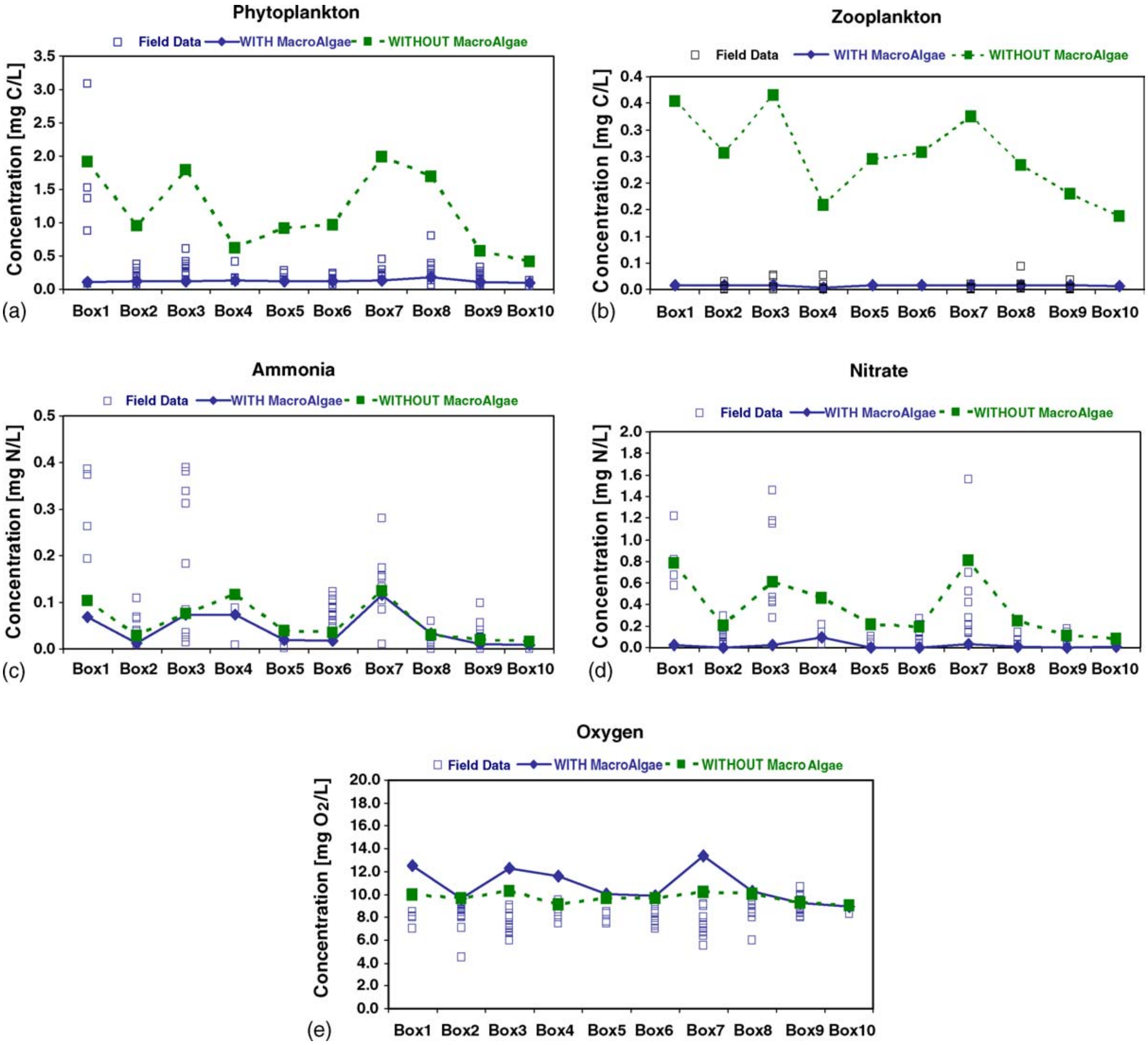

Fig. 4. (a–e) Annual concentration of phytoplankton, zooplankton, ammonia, nitrate and oxygen computed by the model (WITH and WITHOUT macroalgae) and field data measured in the boxes (data measured among 1989–1993, 2000 and 2002).

Fig. 5a–g represents the annual evolution of properties average concentration in the estuary (WITH and WITHOUT macroalgae), for the fifth year of simulation when the model gives stable cyclic evolution profiles. The widths of the lines represent the diurnal variations giving a measure of the temporal variation along a tide cycle. The graphs show significant differences between these two simulations, in all properties.

In agreement with Fig. 4, graphs in Fig. 5 show that phytoplankton and zooplankton concentration in Ria de Aveiro are quite reduced in the presence of macroalgae, mainly because of the large reduction of nitrate in the system. Consequently, the extension of “prey-predator” relation between phytoplankton and zooplankton is reduced too. The major process limiting phytoplankton growth is, now, only the availability of nutrients, having zooplankton predation an insignificant contribution controlling the phytoplankton stock. This can be better verified in Fig. 6 that shows the two organism’s dynamics when considering each scenario separately.

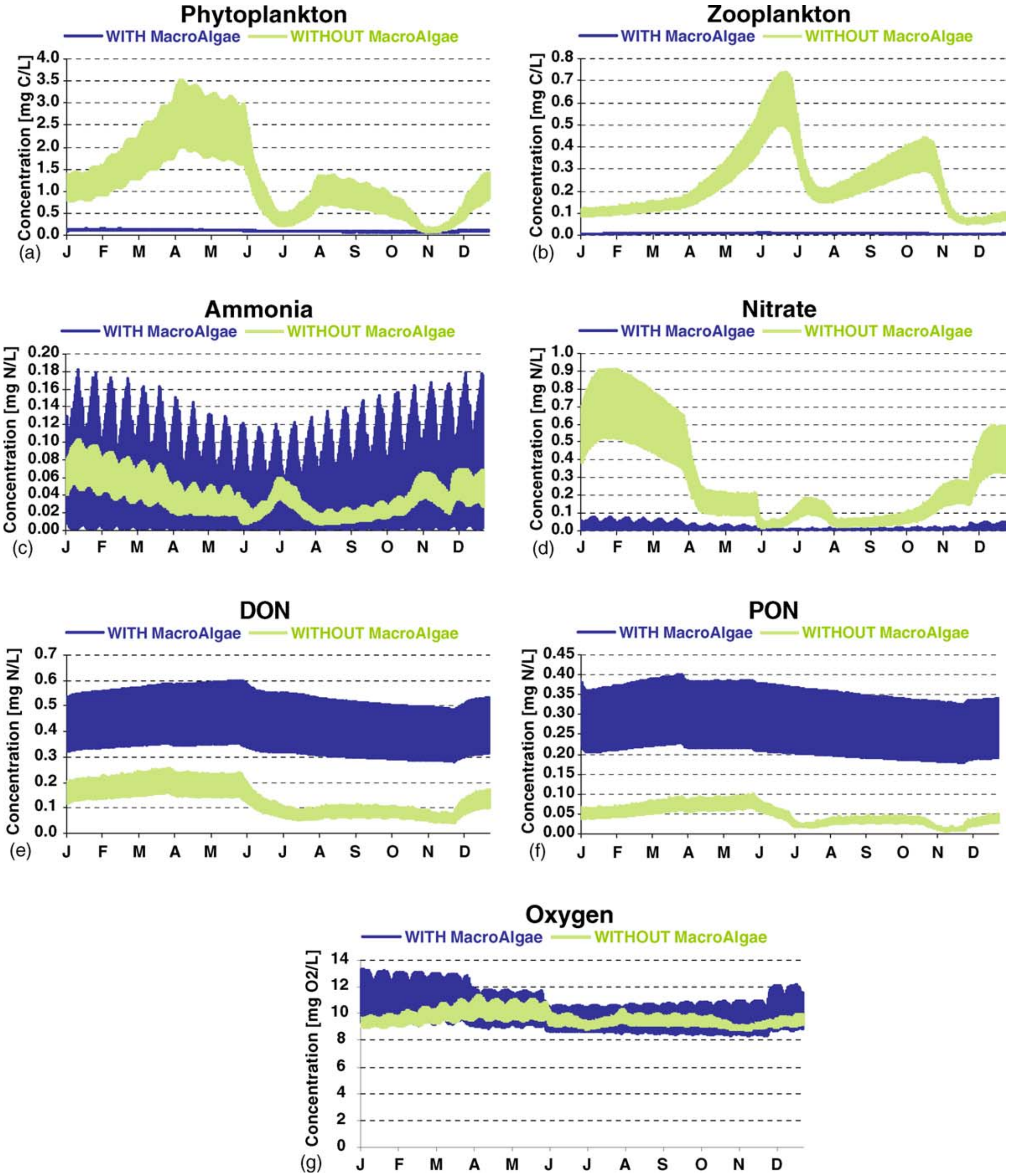

Fig. 5. (a–g) Comparison of the annual evolution of properties spatial average concentration in Ria de Aveiro WITH and WITHOUT macroalgae in model simulations.

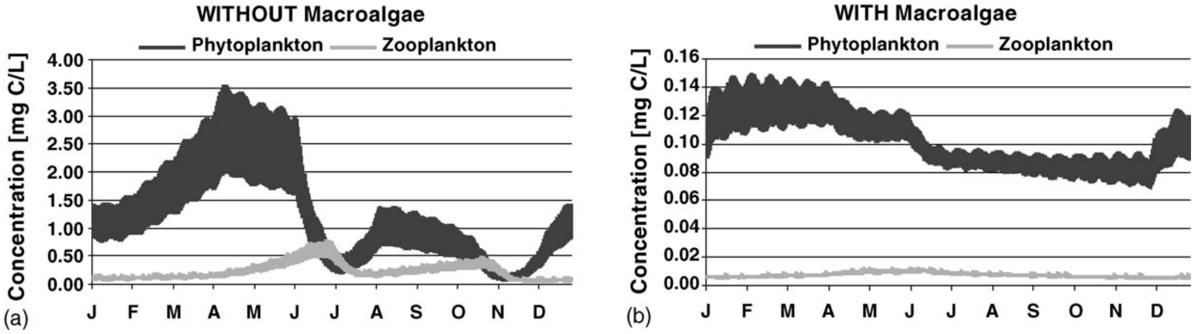

Fig. 6. (a) and (b) Phytoplankton and zooplankton dynamics WITH and WITHOUT macroalgae in model simulations.

With macroalgae in the system, the availability of nutrients in water column is reduced, mostly nitrate (Fig. 5c and d). In terms of ammonia, the existence of another primary producer, leads to more excretion products, accelerating mineralization processes and, for that reason, the ammonia concentration does not decrease strongly, as nitrate. In Fig. 5e and f it is also interesting to notice the increase in DON and PON concentration, in the macroalgae simulation, which indicates the great importance of macroalgae excretions in nutrients dynamics. As expected, there is an increase in the average oxygen concentration (Fig. 5g), not only because there is one more primary producer, but also because macroalgae are attached and cannot be exported off estuary like phytoplankton. One should notice that oxygen gradients are also amplified, leading to the conclusion that the system is more prone to anoxic events.

Fig. 7 represents the evolution of macroalgae average biomass (kgC $m^{-2}$) over 6 years, where is possible to see macroalgae biomass increasing and stabilizing after the fifth year. The low nutrient input in Ria de Aveiro is responsible for the continuous growth but with a negative acceleration. In fact, nutrients availability in the system is the most important limiting factor, as it is shown in Fig. 8. However, phytoplankton concentrations and macroalgae's densities are not high enough to cause a significant self-shading effect (notice the high light limitation factor values in Fig. 8) and thus, net growth is always positive. This means that Ria de Aveiro has particularly special conditions of depth and nutrient dynamics to allow high macroalgae biomass values such as approximately 150 gC $m^{-2}$. To compare, Ferreira (1989) averaged a value of 5 gC $m^{-2}$ for macroalgae biomass in Tagus estuary (Portugal) which is a deep and turbid estuary, causing benthic producers to be mainly limited by light.

From the model results analysis it is also possible to compare the difference between the phytoplankton limitation factors in both simulations. Fig. 9a–c represents the evolution of light and nutrients limitation, and also the total limitation, for phytoplankton growth, which is computed as the multiplication of all factors (light, nutrient and temperature). The limitation caused by temperature is not shown because both simulations have equal conditions and its effect is not significant compared to others.

In MOHID system, phytoplankton growth light limitation factor is computed considering, not only the evolution of the solar radiation along the year (depending on the local coordinates and the sun course), but also the self-shading effect from phytoplankton (see Section 2.2.2). WITH macroalgae, the phytoplankton concen-

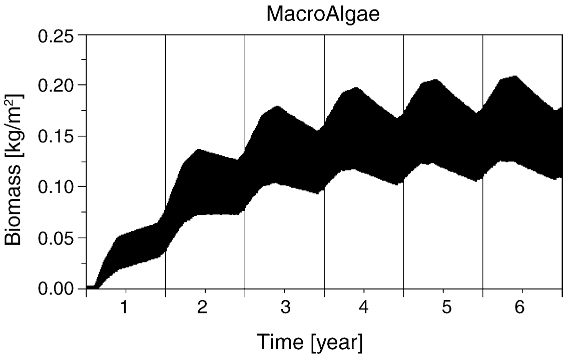

Fig. 7. Macroalgae concentration (kgC $m^{-2}$) evolution, along six consecutive years.

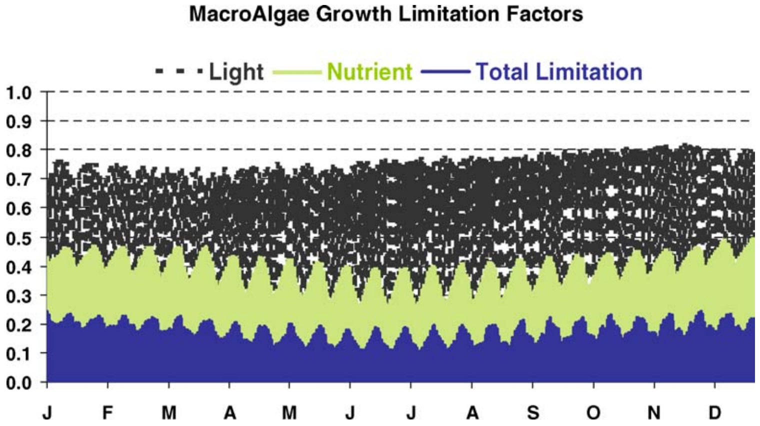

Fig. 8. Macroalgae growth limiting factors during the fifth year of simulation.

trations have a significant diminution in Ria de Aveiro and, consequently, the self-shade effect is reduced, increasing light limitation factor. It is important to notice that WITH macroalgae the seasonal variability of the light limitation factor is not so profound, as a result of no significant variation in phytoplankton concentration (Fig. 6). Nutrients limitation is higher in the presence of macroalgae (which corresponds to lower limitation factors) because macroalgae uptake represents an important sink of nutrients in the system. This result corroborates with the conclusions discussed above, where nutrients were considered as the major factor limiting

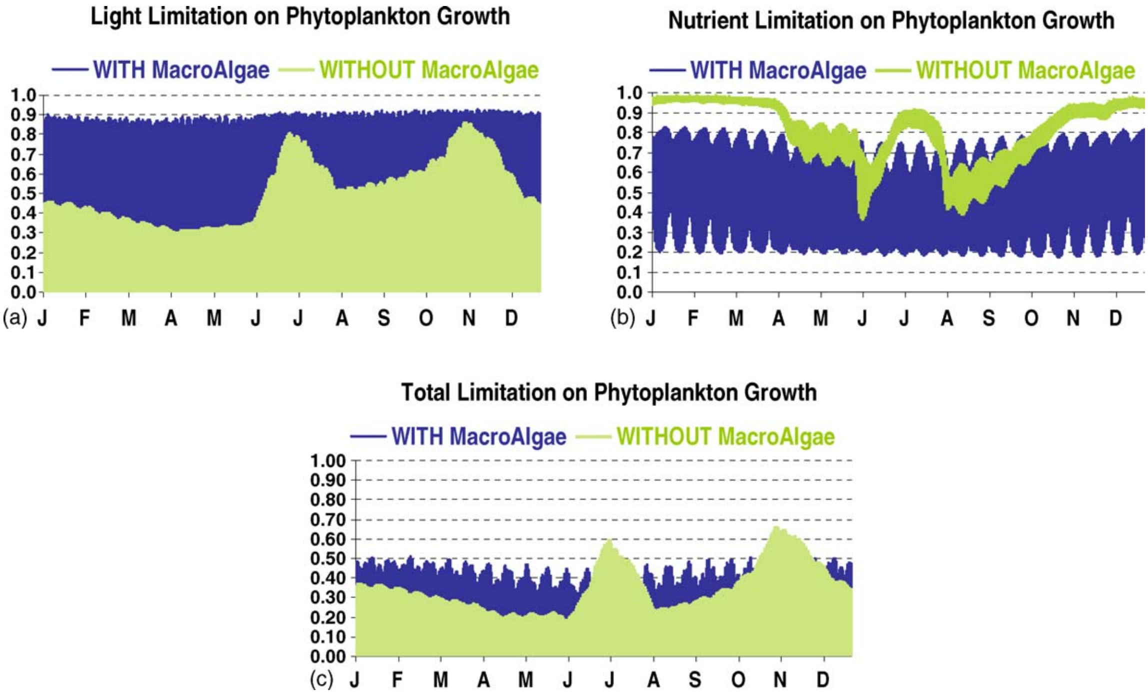

Fig. 9. Factors limiting the phytoplankton growth WITH and WITHOUT macroalgae (fifth year of simulation).

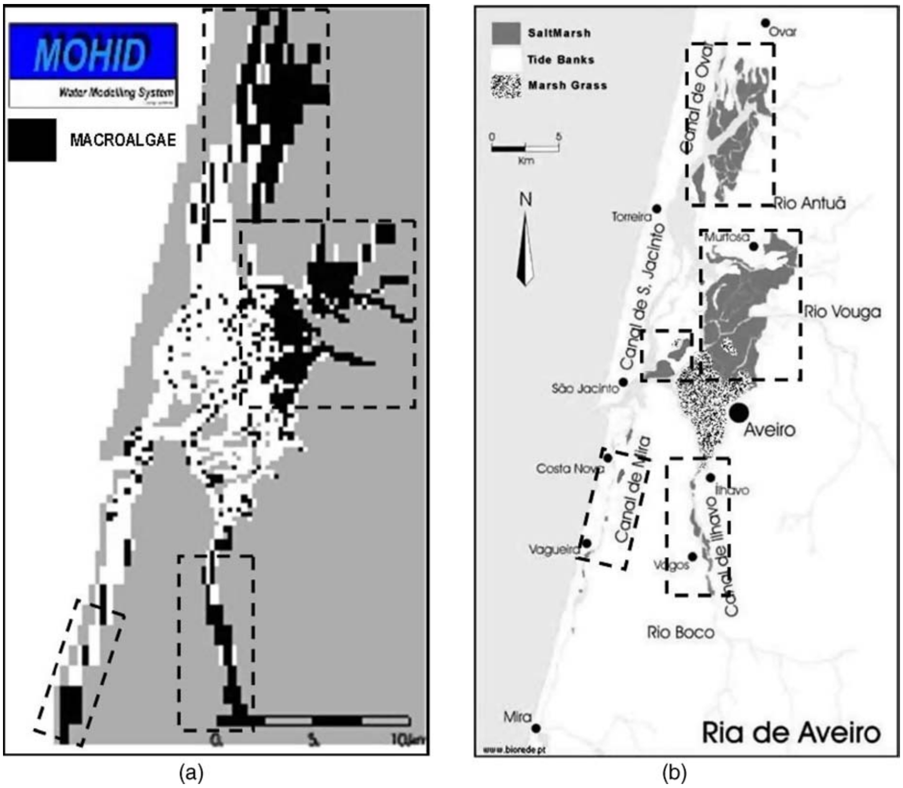

(a) (b)

Fig. 10. (a) Macroalgae distribution in Ria de Aveiro after 6 years of simulation. Dashed boxes emphasize the common areas; (b) SaltMarsh and Marsh Grass distribution in Ria de Aveiro (adapted from www.biorede.pt).

primary production. From the total limitation factor evolution, showed in Fig. 9c, it is possible to conclude that phytoplankton growth is, in average, more limited in the simulation WITH macroalgae, which explains lower values of concentration in Ria de Aveiro (Fig. 5a).

Fig. 10a represents macroalgae distribution in Ria de Aveiro after 6 years of simulation. The model results indicate areas next to rivers discharge as preferential establishment areas for macroalgae, particularly near Caster River discharge, one of the major nutrients contributors in Ria de Aveiro according to ModelRia project field data. The establishment pattern is in accordance with the salt marsh areas presented in Fig. 10b, indicating that the criteria used for macroalgae distribution can be considered as valid.

The fact that the preferential establishment areas (near Caster, Antuã and Boco River discharges) are the ones with higher residence times implies that there is a strong competitive factor between macroalgae and phytoplankton, both for light and nutrients. This can be confirmed by the changes of phytoplankton concentration evolution in the presence of macroalgae (Fig. 6).

## 4. Conclusion

MOHID is a modelling system programmed in an object-oriented philosophy, allowing a simple integration of new simulation properties, such as macroalgae. The model has proved to be flexible in the incorporation of a new simulation property such as macroalgae that has the particularity of being a component of the water quality model not transported by advection or diffusion, and in constant interaction with sediment dynamics. These features enable the dynamic prediction of macroalgae establishment patterns, as well as their productivity rates. In addition, the light extinction formulation used for macroalgae enables the possibility of simulating a wide range of macroalgal morphologic behavioural patterns. The simple and systematic parameterizations used in the water quality model associated with the format of model results (analysis of punctual or spatially integrated results) allow an easy calibration of model results.

In MOHID application to Ria de Aveiro, the results show that the model is better adjusted to field data with macroalgae simulation and that they can have a significant role in primary production. In the presence of macroalgae, phytoplankton biomass production inside Ria de Aveiro was significantly reduced and the total photosynthetic biomass is mainly comprised by macroalgae. The main reason for this greater development of macroalgae, instead of phytoplankton, is the fact that the macroalgae stay inside the estuary for longer time, allowing them to consume more nutrients and produce more biomass, while phytoplankton depends on the transport of water trough Ria de Aveiro and, after 20 days (according to the model results) all phytoplankton inside the estuary will be washout to the ocean. These results show that macroalgae cause a shift in phytoplankton growth limitation. Instead of being limited by zooplankton, phytoplankton is mainly limited by nutrients, due to uptake by macroalgae. This reduction in their biomass allied to an insufficient residence time, decreases the self-shading effect and eliminates light as one of the limitations to primary production in this estuary.

This study, and the developed model itself, can be the first steps in management practices delineation, offering useful tools that can simulate several scenarios, in this estuary as in others.

## Acknowledgements

This research was possible within the framework of a project of Portuguese National Water Institute (INAG) to evaluate Water Quality in Portuguese Estuaries. ModelRia project, financed by the Portuguese Science and Technology Foundation, must also be acknowledged, with special attention to the sampling work made by Prof. Henrique Queiroga. The authors would also like to thank the contributions of two anonymous reviewers.

## Appendix A. Supplementary data

Supplementary data associated with this article can be found, in the online version, at 10.1016/j.ecolmodel.2005.01.054.

## References

Alvera-Azcárate, A., Ferreira, J.G., Nunes, J.P., 2003. Modelling eutrophication in mesotidal and macrotidal estuaries. The role of intertidal seaweeds. Est. Coast. Shelf. Sci. 57, 715–724.

Atkinson, M.J., Smith, S.V., 1983. C:N:P ratios of benthic marine plants. Limnol. Oceanogr. 28, 568–574.

Baird, M.E., Walker, S.J., Wallace, B.B., Webster, I.T., Parlsow, J.S., 2003. The use of mechanistic descriptions of algal growth and zooplankton grazing in an estuarine eutrophication model. Est. Coast. Shelf. Sci. 56 (3/4), 685–695.

Bell, E.C., 1993. Photosynthetic response to temperature and dessication of the intertidal alga *Mastocarpus papillatus*. Mar. Biol. 177, 337–346.

Braunschweig, F., Martins, F., Leitão, P., Neves, R., 2003. A methodology to estimate renewal time scales in estuaries: the Tagus Estuary case. Ocean Dyn. 53 (3), 137–145.

Carr, G., Duthie, H., Taylor, W., 1997. Models of aquatic plant productivity: a review of the factor that influence growth. Aquat. Bot. 59, 195–215.

Cloern, J.E., 2001. Our evolving conceptual model of the coastal eutrophication problem. Mar. Ecol. Prog. Ser. 210, 223–253.

Coelho, H., Santos, R., 2003. Enhanced primary production over seamounts: a numerical study. Thalassas 19 (2a), 144–145.

Coffaro, G., Bocci, M., 1997. Resources competition between *Ulva rigida* and *Zoostera marina*: a quantitative approach applied to the Lagoon of Venice. Ecol. Model. 102, 81–95.

Coffaro, G., Sfriso, A., 1997. Simulation model of Ulva rigida growth in shallow water of the Lagoon of Venice. Ecol. Model. 102, 55–66.

Cunha, M., Coelho, H., Neves, R., Leitão, P.C., 2000. A numerical study of the Guadiana estuary. In: Proceedings of the Third Symposium on the Iberian Atlantic Margin, Faro, Portugal, pp. 27–28.

Day, J.W., Hall, C., Kemp, W., Yáñez-Arancibia, A., 1989. Estuarine Ecology. Wiley, 558 pp.

Dennison, W.C., 1979. Light Adaptations of Plants: A Model Based on the seagrass *Zostera marina*. L.M.S. Thesis. University of Alaska, Fairbanks, 70 pp.

Dias, J., Lopes, J., Dekeyser, L., 1999. Hydrological characterisation of Ria de Aveiro, Portugal, in early Summer. Oceanol. Acta 22, 473–485.

Dronkers, J., Leussen, W., 1988. Physical Processes in Estuaries. Springer-Verlag, Berlin, Germany, 560 pp.

Duarte, P., Ferreira, J.G., 1997. A model for the simulation of macroalgal population dynamics and productivity. Ecol. Model. 98, 199–214.

Enriquez, S., Agustí, S., Duarte, C., 1994. Light absorption by marine macrophytes. Oecologia 98, 121–129.

EPA, 1985. Rates, Constants and Kinetics Formulations in Surface Water Quality Modelling, 2nd ed. United States Environmental Protection Agency, Report EPA/600/3-85/040, 454 pp.

Falkowski, P., 2000. Racionalizing elemental ratios in unicellular algae. J. Phycol. 36, 3–6.

Ferreira, J., 1989. Mercúrio em algas macrófitas do Estuário do Tejo. PhD Dissertation. Environmental Sciences, Universidade Nova de Lisboa, Portugal.

Fonseca, M., Kenworthy, W., 1987. Effects of current on photosynthesis and distribution of seagrasses. Aquat. Bot. 27, 59–78.

Gotelli, N., 1995. A Primer of Ecology. Sinauer Associates Inc., USA, 206 pp.

INAG, 2003. Water Quality in Portuguese Estuaries—Ria de Aveiro, vol. V. Technical Report for Portuguese National Water Institute, Portugal.

Kaandorp, J., Kübler, J., 2001. The Algorithmic Beauty of Seaweeds, Sponges and Corals. The Virtual Laboratory, Springer-Verlag (Chapter 2).

Krone, R., 1962. Flume Studies of the Transport in Estuaries Shoaling Processes. Hydr. Eng. Lab., University of Berkeley, California, USA.

Little, C., Kitching, J.A., 1996. The biology of rocky shores. In: Biology of Habitats. Oxford University Press.

Mann, K., 1982. Ecology of coastal waters—a systems approach. Studies in Ecology, vol. 8. Blackwell Scientific Publications, 322 pp.

Miranda, R., Braunschweig, F., Leitão, P., Martins, F., Santos, A., 2000. MOHID2000—a coastal integrated object oriented model. In: Hydraulic Engineering Software VIII. WIT Press.

Neves, R., Delfino, J., Silva, A., Leitão, P., Leitão, J., Pina, P., Braunschweig, F., Miranda, R., Coelho, H., 2000. Coastal management supported by modelling. Optimising the level of treatment of urban discharges into coastal waters. Conference Paper in Environmental Coastal III. Las Palmas, Canary Islands.

Parsons, T., Takahashi, M., Hargrave, B., 1984. Biological Oceanographic Processes. Butterworths–Heinemann, 330 pp.

Partheniades, E., 1965. Erosion and deposition of cohesive soils. J. Hydr. Div. ASCE 91 (HY1), 105–139.

Pina, P., 2001. An integrated approach to study the Tagus estuary water quality. Master Dissertation. Marine resources ecology, management and modelling. Instituto Superior Técnico, Universidade Técnica de Lisboa, Portugal, 70 pp.

Pina, P., Delfino, J.P., Leitão, P.C., Neves, R.J., 2000. An integrated approach to study the Tagus estuary water quality. In: Proceedings of the Third Symposium on the Iberian Atlantic Margin, Faro, Portugal, pp. 95–96.

Pina, P., Braunschweig, F., Saraiva, S., Santos, M., Neves, R., 2003. The role of physics controlling the eutrophication process in estuaries. Thalassas 19 (2a), 157–158.

Portela, L., 1996. Modelação matemática de processos hidrodinâmicos e de qualidade da água no estuário do Tejo. Dissertação PhD Dissertation. Environmental Engineering, Instituto Superior Técnico, Universidade Técnica de Lisboa, Portugal.

Rivera, 1997. Hydrodynamics, sediment transport and light extinction of Cape Bolinao, Philippine. PhD Dissertation. A.A. Balkema/Rotterdam/Brookfield, 244 pp.

Salomonsen, J., Flindt, M.R., Geertz-Hansen, O., Johansen, C., 1999. Modelling advective transport of Ulva lactuca in the sheltered bay, Møllekrogen, Roskilde Fjord, Denmark. Hydrobiologia 397, 241–252.

Solidoro, C., Pecenik, G., Pastres, R., Franco, D., Dejak, C., 1997. Modelling macroalgae (Ulva rígida) in the Venice lagoon: model structure identification and first parameters estimation. Ecol. Model. 94, 191–206.

Steele, J., 1962. Environmental control of photosynthesis in the sea. Limnol. Oceanogr. 7, 137–150.

Valiela, I., 1995. Marine Ecological Processes, second ed. Springer-Verlag, New York, USA, 686 pp.